Nelson *et al*., Phosphoproteomics reveals conserved nodes and regulation of store-operated calcium entry by AMPK

Appendix

Table of Contents **Page**

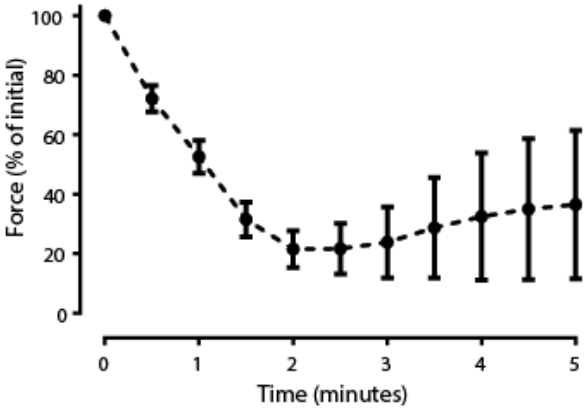

Appendix Figure S1. Contraction force measurements during electrical stimulation of rat tibialis anterior muscle (100 Hz for 5 min; 1 sec on followed by 3 sec off). n=5. Data are represented as mean ± SD. Related to Figure 1.

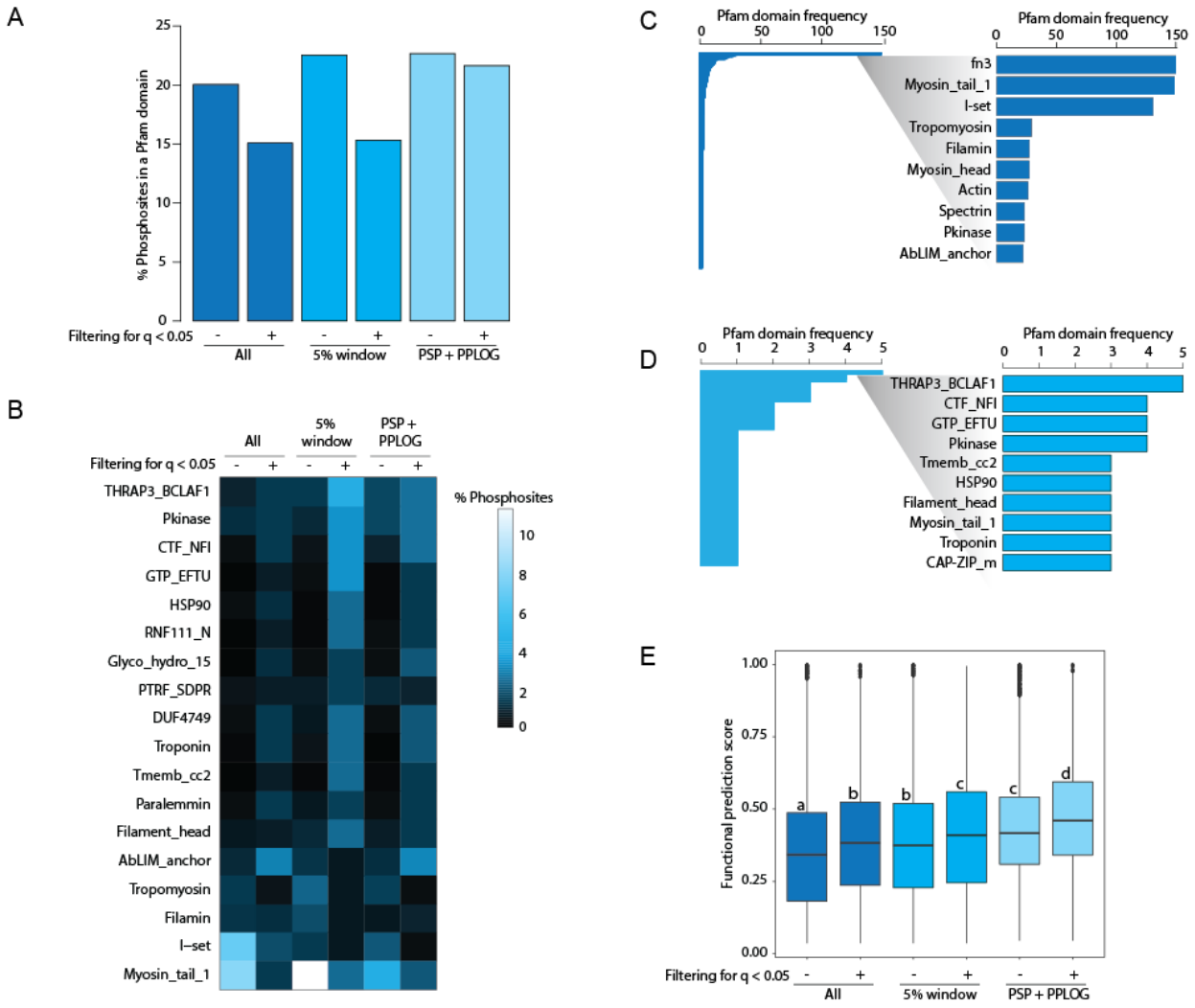

Appendix Figure S2. Orthologous and significantly regulated phosphosites have more frequent attributes of functional phosphosites. **A)** The percentage of phosphosites occurring within a Pfam defined domain. The groups are all identified phosphosites in the human phosphoproteome, phosphosites that fit a 5% window with the rat or mouse datasets and phosphosites with an ortholog in the rat or mouse dataset found by PhosphositePlus or PhosphOrtholog. Further filtering for significantly regulated phosphosites ($q < 0.05$) was also applied to each group. **B)** The percentage of phosphosites in the 10 most common domains from each group. Examples of the distribution and top domains of **C)** all phosphosites and **D)** 5% window-filtered significantly regulated phosphosites. **E)** The functional prediction score (Ochoa et al., 2019) of the separate groups. Welch's ANOVA $p < 0.05$. Groups with the same letter are not significantly different ($p < 0.05$, Games-Howell post-hoc test).

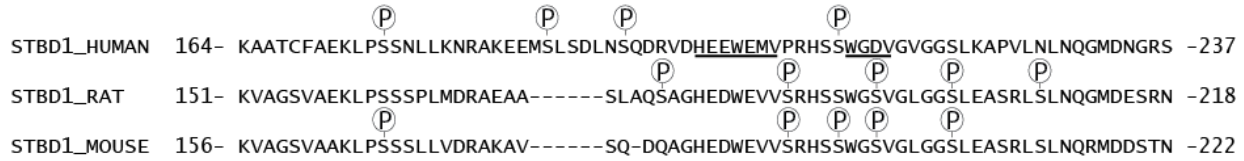

Appendix Figure S3. Human exercise-, rat contraction- or mouse running-regulated phosphosites on Genethonin 1 (starch-binding domain-containing protein 1; STBD1). Underlined is the Atg8 interacting motif (AIM). Related to Figure 2.

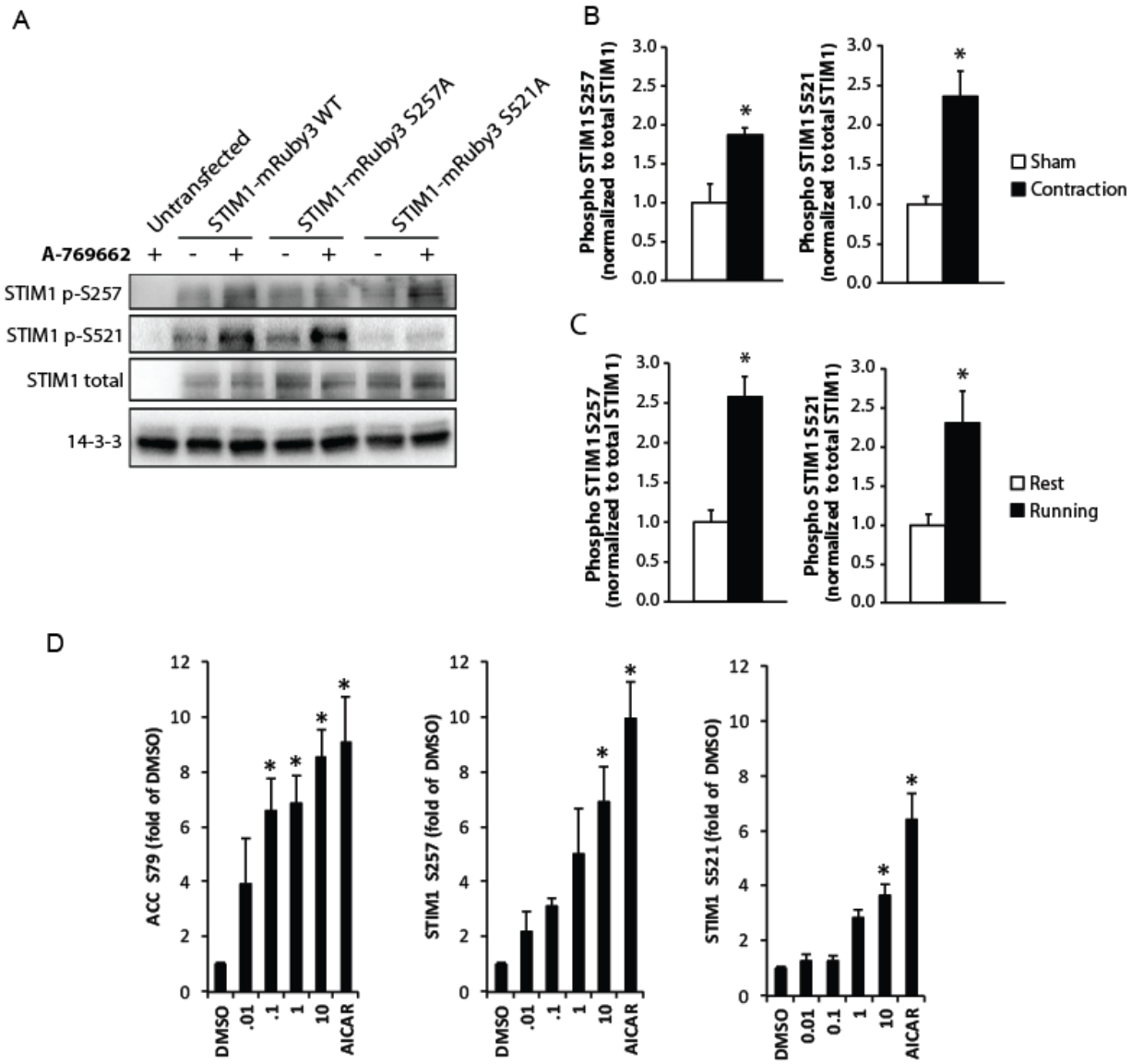

Appendix Figure S4. (A) Western blots for phosphorylated STIM1 (S257 or S521) in HEK-E cells not transfected, or expressing STIM1-mRuby3 WT, S257A or S521A. Cells were treated with the AMPK activator A-769662 (+) or vehicle (-) for 30 min. Total STIM1 was used to determine expression of STIM1-mRuby3 WT or mutants, and 14-3-3 was used as a loading control. Quantification of Western blots from **(B)** rat skeletal muscle subjected to sham or contraction, or **(C)** skeletal muscle from mice subjected to rest or treadmill running. * = $p < 0.05$ for exercise compared to respective control, student's t-test. **(D)** Quantification of Western blots from L6 myoblasts treated with DMSO, increasing concentrations of thapsigargin (.01, .1, 1 or 10 µM), or .5 mM AICAR for 15 min. * = $p < 0.05$ compared to DMSO control, one-way ANOVA with Tukey's post-hoc test. For B-D, data are represented as mean ± SEM. Related to Figure 3.

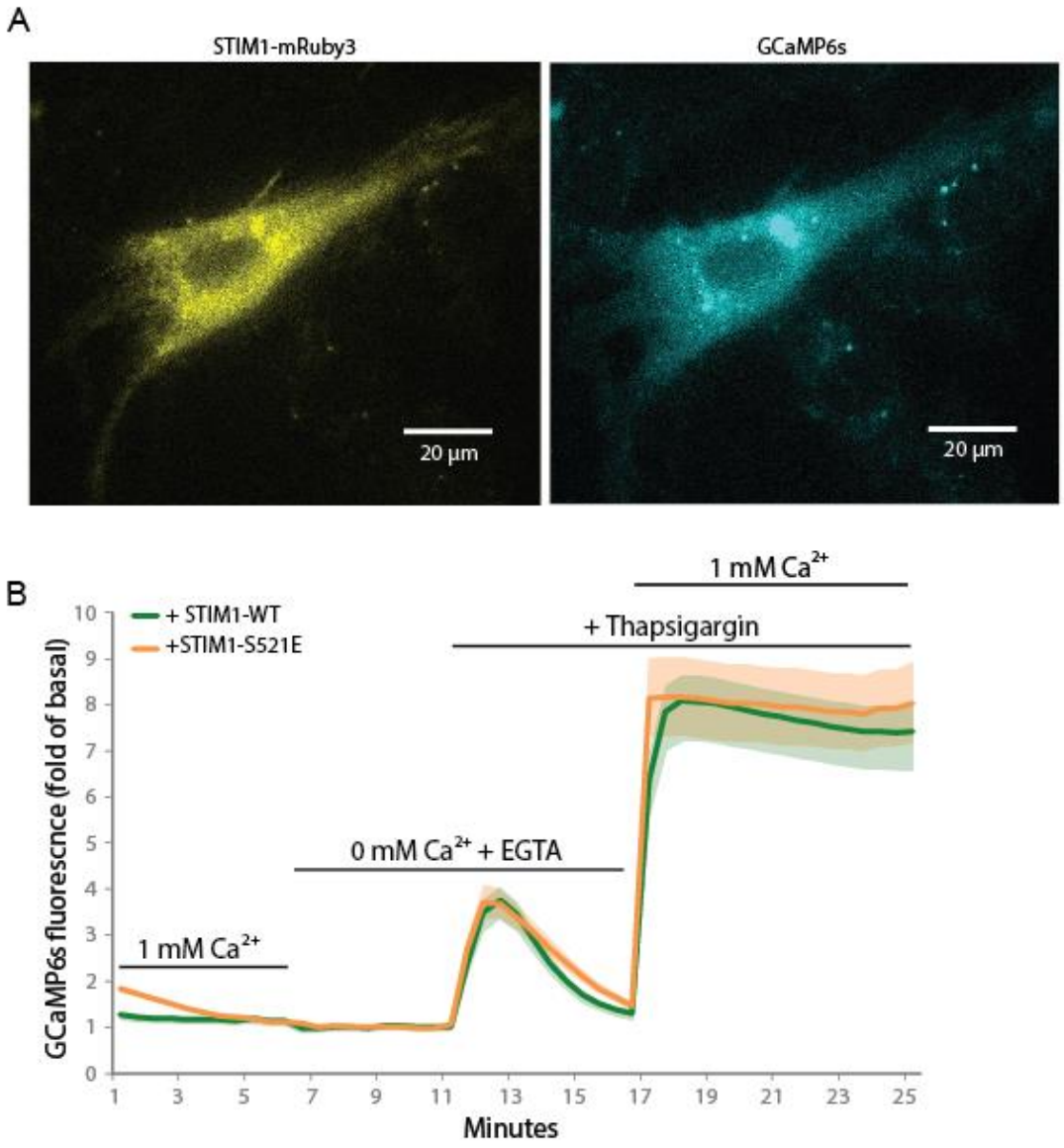
A
STIM1-mRuby3
GCaMP6s
20 µm
20 µm
B
1 mM Ca2+
+ Thapsigargin
+ STIM1-WT
+STIM1-S521E
0 mM Ca2+ + EGTA
1 mM Ca2+
GCaMP6s fluorescnce (fold of basal)
Minutes
C
MAX SOCE (fold of basal)
siSTIM1
+STIM1-WT
+STIM1-S521E
D
mRuby3 expression (raw fluorescence units)
STIM1-WT
STIM1-S257A
STIM1-S257E
STIM1-L251S
STIM1-S521E

Appendix Figure S5. L6 myoblasts were transfected with the genetic cytosolic Ca^{2+} sensor GCaMP6s. Cells were also transfected with siRNA directed at endogenous STIM1 (siSTIM) and full-length wild type (WT) or mutant (S521E) STIM1-mRuby3. **(A)** Representative images of an L6 myoblast co-expressing STIM1-mRuby3 (left) and GCaMP6s (right). **(B)** Ca^{2+} levels over time (fold of 0 mM Ca^{2+} + EGTA basal) and **(C)** quantification of store-operated Ca^{2+} entry in in L6 myoblasts incubated in buffer containing 1 or 0 mM Ca^{2+} and treated with 2 µM thapsigargin during the indicated times. These WT data are duplicated from Figure 5 B-C to compare S521E. **(D)** STIM1-mRuby3 expression measured via fluorescence microscopy. Data are represented as mean ± SEM. Related to Figure 5.

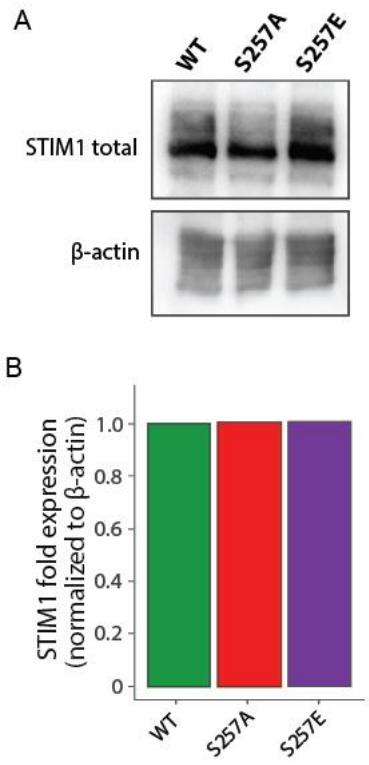

Appendix Figure S6. (A) Western blots and **(B)** quanitification for total STIM1 in STIM whole-body knockout flies overexpressing WT or mutant (S257A or S257E human STIM1-mRuby3. β-actin was used as a loading control. Related to Figure 6.

Appendix Table S1. Conserved exercise-regulated phosphosites.

GeneNames	Human UniProt-Site	Rat UniProt-Site	Mouse UniProt-Site	Human Exercise	Rat Contraction	Mouse Running
AKAP13	Q12802-S2563	F1M3G7-S2511	E9Q394-S2527	▲	▲	▲
ALPK3	Q96L96-S1390	D3ZH28-S1169	D3YUT2-S1165	▼	▲	▼
ALPK3	Q96L96-S1406	D3ZH28-S1185	D3YUT2-S1181	▼	▼	▼
ALPK3	Q96L96-T1409	D3ZH28-T1188	D3YUT2-T1184	▼	▲	▼
AMPD1	P23109-S118	P10759-S85	Q3V1D3-S83	▲	▲	▼
C18orf25	Q96B23-S147	D4A3X1-S147	Q8BH50-S147	▲	▲	▲
C18orf25	Q96B23-S67	D4A3X1-S67	Q8BH50-S67	▲	▲	▲
CAMK2G	Q13555-S311	P11730-S311	Q923T9-S311	▲	▲	▼
CLASP2	O75122-S313	Q99JD4-S319	Q8BRT1-S319	▲	▲	▲
CLCN1	P35523-S886	P35524-S892	Q64347-S892	▲	▲	▼
CRYAB	P02511-S59	P23928-S59	P23927-S59	▲	▲	▲
EIF4B	P23588-S497	Q5RKG9-S497	Q8BGD9-S497	▲	▲	▲
EIF4G1	Q04637-S1097	D3ZU13-S1099	Q6NZJ6-S1101	▼	▼	▲
FAM65A	Q6ZS17-S22	Q4FZU8-S22	Q68FE6-S22	▲	▼	▼
FLNC	Q14315-S2624	D3ZHA0-S2625	Q8VHX6-S2625	▲	▲	▲
GPHN	Q9NQX3-S305	Q03555-S337	Q8BUV3-S338	▲	▲	▲
HNRNPA3	P51991-S116	Q6URK4-S116	Q8BG05-S116	▲	▲	▼
HSPB1	P04792-S15	P42930-S15	P14602-S15	▲	▲	▲
HSPB1	P04792-S82	P42930-S86	P14602-S86	▲	▲	▲
LMOD2	Q6P5Q4-S392	A1A5Q0-S398	Q3UHZ5-S399	▲	▲	▼
LMOD2	Q6P5Q4-S512	A1A5Q0-S514	Q3UHZ5-S515	▼	▼	▼
LMOD2	Q6P5Q4-T384	A1A5Q0-T390	Q3UHZ5-T391	▼	▲	▼
LNPEP	Q9UIQ6-S91	P97629-S91	Q8C129-S91	▲	▲	▲
MAPT	P10636-S713	P19332-S707	P10637-S688	▼	▼	▼
MLLT4	P55196-S1182	O35889-S1189	Q9QZQ1-S1182	▲	▲	▲
MLLT4	P55196-S1275	O35889-S1282	Q9QZQ1-S1275	▼	▼	▼
MTDH	Q86UE4-S298	Q9Z1W6-S297	Q80WJ7-S297	▲	▲	▲
MTFR1L	Q9H019-S103	Q5XII9-S100	Q9CWE0-S100	▲	▲	▲
MTOR	P42345-S1261	P42346-S1261	Q9JLN9-S1261	▲	▲	▲
NDRG2	Q9UN36-S338	Q8VBU2-S338	Q9QYG0-S338	▼	▼	▼
NDRG2	Q9UN36-T330	Q8VBU2-T330	Q9QYG0-T330	▼	▼	▼
NFIX	Q14938-S265	O70189-S1	P70257-S265	▲	▲	▲
NFIX	Q14938-S268	O70189-S4	P70257-S268	▼	▼	▼
OSBPL11	Q9BXB4-S181	B5DF74-S192	Q8CI95-S186	▼	▼	▼
PCM1	Q15154-S1283	G3V7E6-S1280	Q9R0L6-S1280	▲	▲	▲
PDE4A	P27815-S346	P54748-S333	O89084-S333	▲	▲	▼
PDHA1	P08559-S232	P26284-S232	P35486-S232	▼	▼	▼
PHC3	Q8NDX5-S842	D3ZS50-S689	Q8CHP6-S840	▲	▲	▲
PHKA1	P46020-S972	Q64649-S974	P18826-S973	▼	▼	▼
PHLDB1	Q86UU1-S489	D3ZNS1-S490	Q6PDH0-S491	▼	▼	▼
PLEC	Q15149-S4613	P30427-S4616	Q9QXS1-S4620	▼	▼	▼
PNN	Q9H307-S66	D3ZAY8-S66	O35691-S66	▲	▲	▲
PPP1R14A	Q96A00-S26	Q99MC0-S26	Q91VC7-S26	▼	▼	▼
PPP1R3C	Q9UQK1-S33	Q5U2R5-S33	Q7TMB3-S33	▼	▼	▼
PPP2R5A	Q15172-S49	D3ZDI7-S49	Q6PD03-S49	▲	▲	▲
PRKAA2	P54646-S491	Q09137-S491	Q8BRK8-S491	▲	▲	▲
PRKAB2	O43741-S108	Q9QZH4-S107	Q6PAM0-S107	▲	▲	▲
RAPGEF2	Q9Y4G8-S585	F1M386-S585	Q8CHG7-S585	▲	▼	▼
RCSD1	Q6JBY9-S127	F1M4V3-S97	Q3UZA1-S127	▲	▲	▲
RPS6KB2	Q9UBS0-S416	D4AE24-S416	Q9Z1M4-S416	▲	▲	▲
RPTOR	Q8N122-S722	D3ZDU2-S722	Q8K4Q0-S722	▲	▲	▲
SPEG	Q15772-S2109	Q63638-S2114	E9QQ25-S2114	▲	▲	▼
STIM1	Q13586-S257	P84903-S257	P70302-S257	▲	▲	▲
STIM1	Q13586-S521	P84903-S521	P70302-S521	▲	▲	▲
STIM1	Q13586-S575	P84903-S575	P70302-S575	▼	▼	▼
SYNPO2	Q9UMS6-S820	D4A702-S818	Q91YE8-S813	▼	▼	▲
SYNPO2	Q9UMS6-S902	D4A702-S900	Q91YE8-S895	▼	▼	▼
TBC1D1	Q86TI0-S237	D4A4U9-S231	Q60949-S231	▲	▲	▲
TFEB	P19484-S109	Q4KLM8-S168	Q9R210-S108	▼	▼	▼
TNS1	Q9HBL0-S1269	F1LN42-S1442	E9Q0S6-S1423	▼	▼	▼
TNS1	Q9HBL0-S1297	F1LN42-S1470	E9Q0S6-S1451	▼	▼	▼
VAPA	Q9P0L0-S164	Q9Z270-S164	Q9WV55-S164	▲	▲	▼
VAPA	Q9P0L0-S219	Q9Z270-S219	Q9WV55-S219	▲	▲	▼
VIPAS39	Q9H9C1-S121	Q5PQN6-S119	Q8BGQ1-S119	▲	▲	▲
XIRP1	Q702N8-S295	D4ABA9-S294	E9QQ93-S295	▲	▲	▲
XIRP1	Q702N8-S529	D4ABA9-S532	E9QQ93-S533	▲	▲	▲
XIRP1	Q702N8-S684	D4ABA9-S687	E9QQ93-S688	▲	▲	▲